Polym. Bull. (2012) 69:137–147
DOI 10.1007/s00289-011-0693-7

ORIGINAL PAPER

Postfunctionalization of aromatic polyamine by [2+2] cycloaddition of 7,7,8,8-tetracyanoquinodimethane with side chain alkynes

Yusuke Washino · Kimie Murata ·
Tsuyoshi Michinobu

Received: 15 September 2011 / Revised: 21 October 2011 / Accepted: 12 December 2011 /

Abstract Electron-rich, side chain alkynes of an aromatic polyamine were functionalized by a [2+2] cycloaddition, followed by retro-cyclization with the electron-accepting 7,7,8,8-tetracyanoquinodimethane (TCNQ). ^{1}H NMR studies were used to optimize the reaction conditions. Mild heating to >50 °C afforded the post-functionalized aromatic polyamines with the desired acceptor amounts. The quantitative TCNQ addition was demonstrated by the MALDI-TOF mass spectrum and elemental analysis. Introduction of the cyano-based acceptor moieties into the polymer side chains resulted in unusually strong intermolecular interactions. In addition to the π–π interactions of the extended acceptor moieties, these intermolecular forces were supposed to improve the thermal stability of the aromatic polymers. Furthermore, the donor–acceptor chromophores formed by this post-functionalization displayed low energy charge-transfer bands and redox activities in both the anodic and cathodic directions. The straightforward postfunctionalization technique using the alkyne–TCNQ addition is useful for the preparation of narrow band gap polymers in one step.

Y. Washino
Department of Organic and Polymeric Materials, Tokyo Institute of Technology, 2-12-1 Ookayama,
Meguro-ku, Tokyo 152-8552, Japan

K. Murata · T. Michinobu (✉)
Global Edge Institute, Tokyo Institute of Technology, 2-12-1 Ookayama, Meguro-ku,
Tokyo 152-8550, Japan
e-mail: michinobu.t.aa@m.titech.ac.jp

T. Michinobu
PRESTO, Japan Science and Technology Agency (JST), Kawaguchi, Japan

Keywords Aromatic polyamine · Charge transfer · Electrochemistry · Postfunctionalization

Introduction

Organic semiconducting polymers are an important class of materials for the realization of solution processible, low-cost and large area electronics [1]. Examples include aromatic polyamines for hole-transporting layers in organic light-emitting devices (OLEDs) [2–4], regio-regular poly(3-alkylthiophene)s for *p*-type semiconductors in photovoltaic cells (PCs) [5, 6], and donor–acceptor type conjugated polymers for ambipolar type thin film transistors (TFTs) [7–10]. In contrast to a large number of p-type semiconducting polymers, there are few guidelines for constructing n-type polymers. Poly(benzobisimidazobenzophenanthroline) (BBL) is a commercially available n-type polymer, which shows an electron mobility (μ_e) of 0.1 $cm^2 V^{-1} s^{-1}$ [11]. However, this polymer has a solubility problem due to its highly rigid ladder structure. It was recently demonstrated that thiophene-based conjugated polymers possessing imide moieties in the conjugated main chain display n-channel TFT performances [12]. This successful result was achieved by the careful selection of monomer structures on the basis of computational modeling. These recent studies suggest that there is still room for pursuing new semiconducting polymers with controlled energy levels.

We have been trying to develop an experimental technique to control the polymer energy levels by adapting semiconducting polymer doping techniques [13–20]. The key reagent of this project is cyano-containing strong acceptor molecules, which are originally p-type doping reagents, but undergo [2+2] cycloaddition with electron-donor-activated alkynes [21, 22]. The cyclobutene intermediates formed by the [2+2] cycloaddition are smoothly transformed into donor–acceptor type products via ring opening. The important features of this reaction are high efficiency, no byproducts, and easy purification without chromatographic techniques, which are also the main criteria of “click chemistry” [23]. For example, when one of the most compact acceptor molecules, tetracyanoethylene (TCNE), was added to a solution of the side chain alkyne-appended aromatic polyamine, the reaction quantitatively proceeded at room temperature and an intense red color ascribed to the intramolecular charge transfer of the product occurred [24]. In other words, the LUMO level of the aromatic polyamine was lowered by this postfunctionalization reaction. It is important to note that there was a clear correlation between the polymer LUMO level and the added TCNE amount. A similar result was observed for the postfunctionalization of polythiophene derivatives [25]. This study also suggested that the use of stronger acceptor molecules, such as 7,7,8,8-tetracyanoquinodimethane (TCNQ) and its derivatives [26–34], is effective for the dramatic lowering of the LUMO levels or the enhancement of the n-type characteristics.

Based on these previous studies, we decided to apply the alkyne–TCNQ addition reaction to the postfunctionalization of the aromatic polyamine to create potent n-type polymers. The energy level decrease of the polyamine, as elucidated by its electrochemical redox potentials, was significant when compared to the TCNE-adducted case. The enhanced thermal stability by this postfunctionalization is also described.

Experimental

Materials

Chemicals were purchased as reagent grade from Kanto, Tokyo Kasei, and Aldrich. The synthesis of **P1** was previously reported [24].

General measurements

^1H and ^{13}C NMR spectra were measured on a JEOL model AL300 spectrometer at 20 °C. Chemical shifts are reported in ppm downfield from $SiMe_4$, using the solvent's residual signal as an internal reference. Infrared (IR) spectra were recorded on a JASCO FT/IR-4100 spectrometer. MALDI-TOF mass spectra were measured on a Shimadzu AXIMA-CFR mass spectrometer. The operation was performed at an accelerating potential of 20 kV by a linear positive ion mode with dithranol as a matrix. Gel permeation chromatography (GPC) was measured on a JASCO system (PU-980, CO-965, RI-930, UV-970, and AS-950) equipped with polystyrene gel columns using THF as an eluent at the flow rate of 1.0 mL min^{-1} after calibration with standard polystyrenes. Elemental analysis was performed on a PerkinElmer 2400-Series H CHNS/O analyzer. Thermogravimetric analysis (TGA) was carried out on a Seiko SII TG/DTA 6200, at the heating rate of 10 °C min^{-1} between 20 °C and 500 °C. Differential scanning calorimetry (DSC) measurements were carried out on a Seiko SII DSC 6220 with a Seiko SII EXSTAR 6000 PC Station. UV–Vis–near infrared (NIR) spectra were recorded on a JASCO V-670 spectrophotometer. Fluorescence spectra were recorded on a JASCO FP6500 spectrophotometer. Cyclic voltammograms (CVs) were measured at 20 °C in a classical three-electrode cell. The working, reference, and auxiliary electrodes were a glassy carbon disk electrode (0.07 cm^2), $Ag/Ag^+/CH_3CN/(nC_4H_9)_4NClO_4$, and Pt wire, respectively. All potentials were referenced to the ferrocene/ferricinium (Fc/Fc^+) couple used as an internal standard.

Synthesis

To a solution of **P1** (15 mg) in 1,2-dichloroethane (30 mL), a desired amount of TCNQ solution in 1,2-dichloroethane (1.5–1.7 mM) was added. After the mixture was stirred for 24 h at 80 °C, the solvent was removed in vacuo.

P2 ($x + y = 1$): ^1H NMR (300 MHz, C_6D_6): $\delta = 0.80–1.24$ (m, 30n H), 1.77 (br s, 4n H), 2.34–2.54 (m, 6n H), 6.23 (br s, 4n H), 6.75–7.75 ppm (m, 14n H); IR (KBr): $\nu = 2925, 2852, 2205, 1579, 1560, 1543, 1521, 1508, 1499, 1491, 1464, 1439, 1373, 1313, 1273, 1175, 942, 862, 819, 669$ cm^{-1}; Elemental analysis: calcd for $(C_{57}H_{58}N_6)_n$: C 82.77, H 7.07, N 10.16; found: C 82.30, H 7.16, N 9.70%.

Results and discussion

Postfunctionalization

The precursor polyamine **P1** was prepared by the Pd-catalyzed polycondensation between 2,7-dibromo-9,9-dioctylfluorene and a tolane-based aniline monomer [24]. The side chain alkynes were activated by both the terminal dimethylanilino groups and the main chain triarylamino moieties. Therefore, the postfunctionalization by TCNQ addition was first attempted in 1,2-dichloroethane at room temperature. However, in contrast to the TCNE addition, the reaction with TCNQ was slow. Mild heating to 50 °C gradually changed the solution color from yellow to green, suggesting the formation of donor–acceptor chromophores (Scheme 1). After the sufficient thermal stability of the products was confirmed (vide infra), the TCNQ adducts were prepared at 80 °C. It should be noted that the formed chromophores are regioisomeric mixtures, depending on the TCNQ orientation during the [2+2] cycloaddition reaction.

The postfunctionalization reaction was monitored by its ^{1}H NMR spectra (Fig. 1). A mixture of **P1** and an equivalent amount of TCNQ was dissolved into C_6D_6 and heated to 50 °C. As TCNQ was added to the polymer side chains, a new peak ascribed to the cyclohexa-1,4-diene rings appeared at 6.23 ppm. This peak intensity gradually increased and finally saturated after 24 h. The peak splitting of the methyl groups at 2.3–2.5 ppm supported the presence of the regioisomeric donor–acceptor moieties (vide supra). Also, peak broadening occurred as more TCNQ was added. This was never observed in the case of the TCNE addition, and accordingly, the bulky side chain chromophores probably induced the steric hindrance. In accordance with this observation, no clear peaks especially in the aromatic region were detected in the ^{13}C NMR spectra of **P2**. The NMR experiments demonstrated the utility of this reaction in various research fields. Commercial reagent grade solvents can be employed without further purification. Additionally, a small amount of impurities, such as contaminated oxygen and water, do not interfere with the cycloaddition reaction, as shown by the water impurity in Fig. 1.

The IR spectra also supported the postfunctionalization of **P1** by the TCNQ addition. The weak vibrational peak at 2,209 cm^{-1} ascribed to the C$\equiv$C moieties of

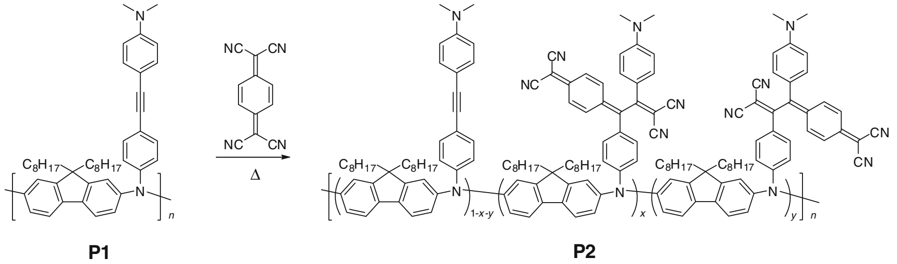

Scheme 1 TCNQ addition to the side chain alkynes of **P1**

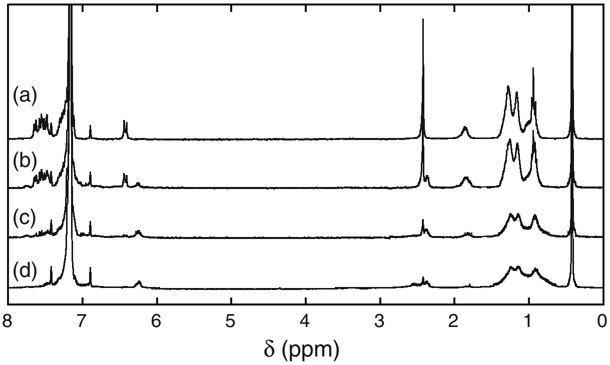

Fig. 1 Reaction progress of **P1** (2.85 mM repeat unit^{-1}) and TCNQ monitored by ^{1}H NMR spectra in C_6D_6 at 50 °C (*a*, 0 h; *b*, 10 h; *c*, 17.5 h; *d*, 24 h). The peak at 0.4 ppm is ascribed to water

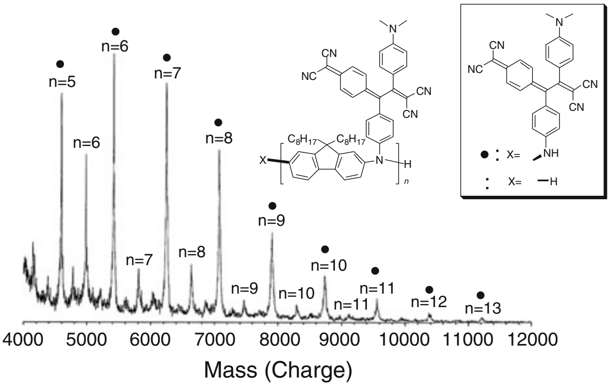

Fig. 2 MALDI-TOF mass spectrum of **P2** ($x + y = 1$) (matrix: dithranol)

P1 was replaced by the C≡N vibrational one centered at 2,205 cm^{-1}. The intensity of the new C≡N peak increased as more TCNQ was added. Moreover, the MALDI-TOF mass spectrum and elemental analysis of **P2** ($x + y = 1$) provided strong evidence of the quantitative addition without any side reactions. Two sets of polymer peak profiles were detected for **P2** ($x + y = 1$) (Fig. 2). The observed peak values and the intervals were in good agreement with the calculated molecular weights of the polymer structures. Molecular masses exceeding 10,000 were not clearly detected due to the limited performance of the instrument. The triangular set of peaks suggested that the termination process of the precursor polymer synthesis is debromination and concomitant hydrogenation. Also, the C, H, and N contents of **P2** ($x + y = 1$) determined from the elemental analysis showed excellent agreement with the calculated values (see "Experimental"). All these results strongly support the quantitative TCNQ addition to **P1**.

Although the MALDI-TOF mass spectrum demonstrated the clean postfunctionalization by TCNQ addition, the GPC profiles showed a different behavior.

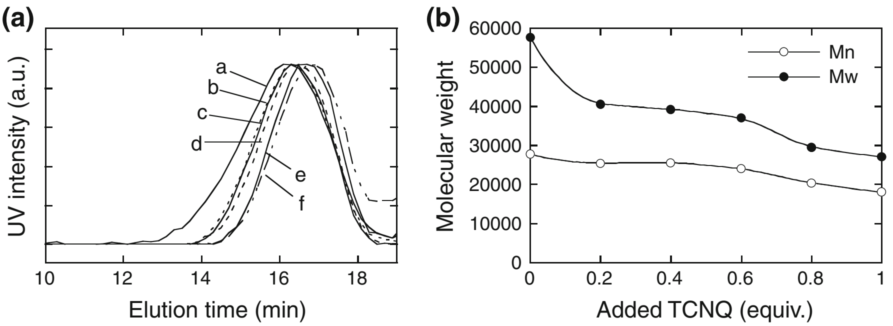

Fig. 3 **a** GPC charts of (*a*) **P1**, (*b*) **P2** ($x + y = 0.2$), (*c*) **P2** ($x + y = 0.4$), (*d*) **P2** ($x + y = 0.6$), (*e*) **P2** ($x + y = 0.8$), (*f*) **P2** ($x + y = 1$) and **b** the calculated number-average and weight-average molecular weights (M_n and M_w) of the polyamines with different TCNQ addition amounts

The number-average (M_n) and weight-average (M_w) molecular weights of **P1**, determined by GPC (THF eluent) in comparison to the calibrated standard polystyrenes, were 27,700 and 57,600, respectively (Fig. 3a). However, the M_n and M_w values estimated from the GPC charts of **P2** gradually decreased with the increasing amount of the TCNQ addition, finally reaching the M_n of 18,000 and M_w of 27,000 for **P2** ($x + y = 1$) (Fig. 3b). A similar decrease in the GPC molecular weights was previously reported for the postfunctionalization of the polystyrene derivatives bearing side chain alkynes [35–37]. These results clearly suggest the strong adhesive feature of the cyano-containing chromophores to polystyrene gels. The adhesive property of the TCNQ adducts is most likely stronger than that of the TCNE adduct. Therefore, it is significant to consider the absolute molecular weights when the degree of postfunctionalization is evaluated.

Thermal analyses

As suggested from the GPC elution curves, the cyano-containing chromophroes induce strong dipolar-based intermolecular forces. It is previously reported that these molecular aggregation features lead to an enhancement of the polymeric thermal properties [38]. For example, the full TCNE addition to **P1** improved the thermal decomposition temperature (T_d) by 118 °C (291 °C → 409 °C) and glass transition temperature (T_g) by 27 °C (125 °C → 152 °C) [24]. In order to elucidate the difference between the TCNE and TCNQ, TGA and DSC measurements of **P2** were performed under nitrogen at the scanning rate of 10 °C min^{-1}. Figure 4a depicts the TGA curves of both **P1** and **P2** ($x + y = 1$). It is apparent that the TCNQ addition is effective for improving the thermal stability. The T_d value of **P2** ($x + y = 1$) was 363 °C, which is significantly higher than that of **P1**, but slightly lower than that of the TCNE adduct. However, the residual soot amount of **P2** ($x + y = 1$) at 500 °C was 68%, which is approximately 6% greater than that of the TCNE adduct. Similar to the TGA results, the T_g values were also investigated by evaluating the second heating scans of the DSC curves. Since **P2** ($x + y = 1$) did not exhibit any noticeable transition peaks, the TCNQ addition amount ($x + y$) was

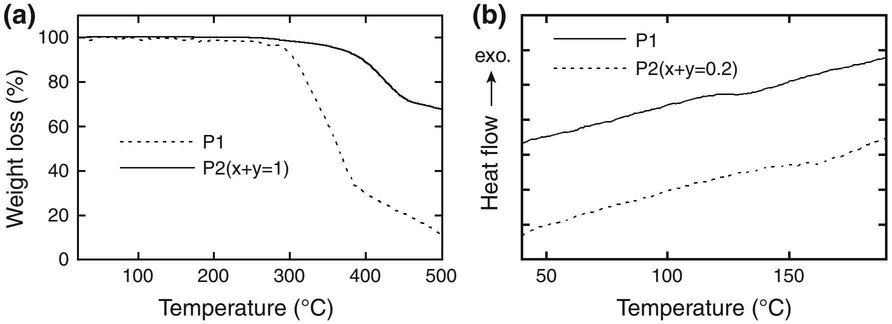

Fig. 4 **a** Thermogravimetric analysis (TGA) curves of **P1** and **P2** ($x + y = 1$) under nitrogen flow at the heating rate of 10 °C min^{-1} and **b** differential scanning calorimetry (DSC) curves of **P1** and **P2** ($x + y = 0.2$) under nitrogen flow at the scanning rate of 10 °C min^{-1}

reduced. The sample **P2** ($x + y = 0.2$) finally displayed the T_g of 150 °C (Fig. 4b), a value that is almost comparable to the full TCNE adduct. Collectively, this result suggested that the thermal improvement ability of the TCNQ adduct with the extended π-system is somewhat better than that of the compact TCNE adduct.

Optical properties

Postfunctional TCNQ addition led to a dramatic change in their optical spectra due to the formation of the donor–acceptor chromophores. The precursor polyamine **P1** possessed the lowest energy absorption maximum (λ_{max}) at 403 nm in 1,2-dichloroethane (Fig. 5). When TCNQ was added to the polymer side chains, new low energy peaks with the λ_{max} of 669 nm appeared and this peak intensity increased in proportion to the added TCNQ amount. The presence of an isosbestic point supported the absence of any side reactions, which was already demonstrated by the MALDI-TOF mass spectrum and elemental analysis (vide supra). The position of the λ_{max} or charge-transfer (CT) band is caused by the combination of the donor and acceptor structures. Due to the more extended π-system of TCNQ, the

Fig. 5 UV–Vis–NIR spectra of **P1** and **P2** with different TCNQ-adducted amounts in 1,2-dichloroethane

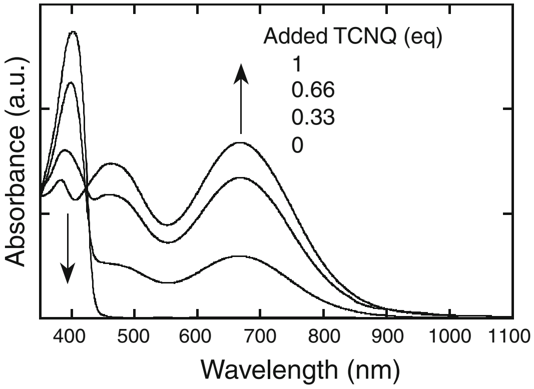

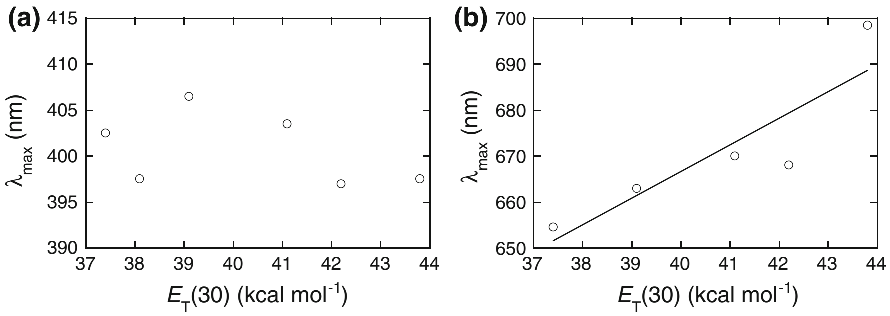

Fig. 6 Relationship between the solvent polarity parameter $E_T(30)$ (tetrahydrofuran, 37.4; ethyl acetate, 38.1; chloroform, 39.1; dichloromethane, 41.1; acetone, 42.2; *N*,*N*-dimethylformamide, 43.8) and the λ_{max} values of **a** **P1** and **b** **P2** ($x + y = 1$)

λ_{max} bathochromically shifted relative to the TCNE-adduct and the end absorption reached into NIR. However, due to the twisted donor–acceptor systems, the TCNQ-adducted polymers were only slightly fluorescent.

In order to highlight the difference in the optical properties after postfunctionalization, the absorption spectra of **P1** and **P2** ($x + y = 1$) were measured in various organic solvents, and the λ_{max} values were plotted as a function of solvent polarity $E_T(30)$ (Fig. 6). The precursor polyamine **P1** revealed no relationship between the absorption spectra and solvent polarity. However, similar to some small molecules and polymers containing this class of donor–acceptor chromophores [39, 40], **P2** ($x + y = 1$) displayed a clear positive solvatochromism. This result indicates the greater dipole moment for **P2**, which is the origin of high performance nonlinear optics [41].

Electrochemistry

A change in both the HOMO and LUMO levels by this postfunctionalization was evaluated by cyclic voltammetry (CV) in CH_2Cl_2 with 0.1 M $(nC_4H_9)_4NClO_4$ at 20 °C. It is reported that the CV of **P1** displays only reversible oxidation steps with the first oxidation potential ($E_{ox,1}$) of 0.10 V (vs. Fc/Fc$^+$) [24]. This $E_{ox,1}$ value corresponds to the HOMO level of −4.90 eV based on the assumption of the Fc/Fc$^+$ couple = −4.80 eV. For the TCNE addition, a gradual decrease in the polymer energy levels had been realized by the addition amount [24]. On the other hand, a small amount of TCNQ addition significantly lowered the energy levels, especially the LUMO level. Consequently, it was difficult to tune the energy levels of **P1** using TCNQ. Figure 7 shows the typical CV curve of **P2** ($x + y = 1$), accounting for the reversible oxidation and reduction peaks ascribed to the aromatic amino donor and TCNQ-based acceptor moieties, respectively. Due to the strong adhesive feature of **P2** onto the working electrode, the anodic and cathodic measurements were conducted separately. The $E_{ox,1}$ of **P2** ($x + y = 1$) was anodically shifted to 0.37 V compared to **P1** because of the efficient intramolecular donor–acceptor interactions. The first reduction potential ($E_{red,1}$) of **P2** ($x + y = 1$) was clearly detected at

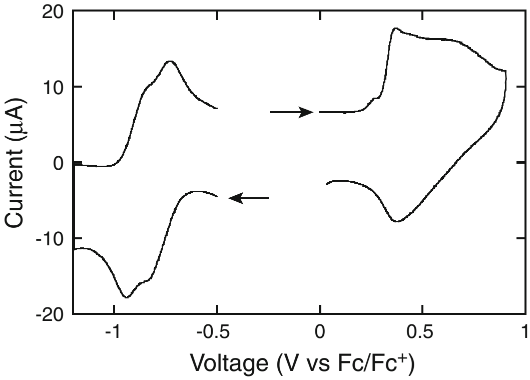

Fig. 7 Cyclic voltammogram of **P2** ($x + y = 1$) in CH_2Cl_2 with 0.1 M $(nC_4H_9)_4NClO_4$ at the scanning rate of 0.1 V s^{-1} under nitrogen

−0.77 V. This potential is comparable to those of the small donor–acceptor molecules [42–44], indicating that the side chain chromophores of **P2** are almost independent of each other. This is probably caused not only by the sp^3-hybridized nitrogen atoms in the polymer main chain, but also by the significant twist between the repeating units. The HOMO and LUMO levels of **P2** ($x + y = 1$) calculated from the redox potentials were −5.17 and −4.03 eV, respectively. The electrochemical band gap (1.14 V in CH_2Cl_2) was consistent with the optical band gap determined by the end absorption (1,034 nm; 1.20 eV in 1,2-dichloroethane).

Conclusion

The clean postfunctionalization of the aromatic polyamine was achieved by the alkyne–TCNQ addition reaction. The quantitative reaction without any side products was demonstrated by a series of analytical methods including MALDI-TOF mass and elemental analyses. The postfunctionalized polyamines displayed significantly lowered energy levels elucidated by the electrochemical redox potentials. In particular, the dramatic decrease in the LUMO level led to the narrow band gap polymers with the electrochemical band gap of 1.14 eV. Further lowering of the LUMO levels or enhancement of the n-type characteristics will be possible through this postfunctional methodology using fluorinated TCNQ derivatives. Application of these n-type polymers to organic electronic devices is also worthwhile for future studies.

Acknowledgments This work was supported, in part, by a Grant-in-Aid for Scientific Research from the Ministry of Education, Science, Sports and Culture, Japan.

References

1. Heeger AJ (2010) Semiconducting polymers: the third generation. Chem Soc Rev 39:2354–2371
2. Shirota Y, Kageyama H (2007) Charge carrier transporting molecular materials and their applications in devices. Chem Rev 107:953–1010
3. Pu YJ, Soma M, Kido J, Nishide H (2001) A novel triphenylamine-substituted poly(*p*-phenylene-vinylene): improved photo- and electroluminescence properties. Chem Mater 13:3817–3819

4. Michinobu T, Kumazawa H, Otsuki E, Usui H, Shigehara K (2009) Synthesis and properties of nitrogen-linked poly(2,7-carbazole)s as hole-transport material for organic light emitting diodes. J Polym Sci Part A Polym Chem 47:3880–3891
5. Yokozawa T, Yokoyama A (2009) Chain-growth condensation polymerization for the synthesis of well-defined condensation polymers and π-conjugated polymers. Chem Rev 109:5595–5619
6. Osaka I, McCullough RD (2008) Advances in molecular design and synthesis of regioregular polythiophenes. Acc Chem Res 41:1202–1214
7. Zaumseil J, Sirringhaus H (2007) Electron and ambipolar transport in organic field-effect transistors. Chem Rev 107:1296–1323
8. Tsuchiya K, Sakakura T, Ogino K (2011) Synthesis of triphenylamine copolymers and effect of their chemical structures on physical properties. Macromolecules 44:5200–5208
9. Michinobu T, Okoshi K, Osako H, Kumazawa H, Shigehara K (2008) Band-gap tuning of carbazole-containing donor-acceptor type conjugated polymers by acceptor moieties and π-spacer groups. Polymer 49:192–199
10. Michinobu T, Osako H, Murata K, Shigehara K (2010) Blue, green, and red light emission of 1,8-carbazole-based conjugated polymers. Chem Lett 39:168–169
11. Babel A, Jenekhe S (2003) High electron mobility in ladder polymer field-effect transistors. J Am Chem Soc 125:13656–13657
12. Letizia JA, Salata MR, Tribout CM, Facchetti A, Ratner MA, Marks TJ (2008) n-Channel polymers by design: optimizing the interplay of solubilizing substituents, crystal packing, and field-effect transistor characteristics in polymeric bithiophene-imide semiconductors. J Am Chem Soc 130:9679
13. Michinobu T (2010) Click synthesis of donor-acceptor-type aromatic polymers. Pure Appl Chem 82:1001–1009
14. Michinobu T (2011) Adapting semiconducting polymer doping techniques to create new types of click postfunctionalization. Chem Soc Rev 40:2306–2316
15. Michinobu T, Kumazawa H, Noguchi K, Shigehara K (2009) One-step synthesis of donor-acceptor type conjugated polymers from ferrocene-containing poly(aryleneethynylene)s. Macromolecules 42:5903–5905
16. Michinobu T, Fujita H (2010) Postfunctionalization of alkyne-linked conjugated carbazole polymer by thermal addition reaction of tetracyanoethylene. Materials 3:4773–4783
17. Li Y, Hyakutake T, Michinobu T (2011) Oxygen permeability change of polyphenylacetylene derivatives by postfunctional TCNE addition. Chem Lett 40:570–572
18. Wang D, Michinobu T (2011) One-step synthesis of ladder-type fused poly(benzopentalene) derivatives with tunable energy levels by variable substituents. J Polym Sci A Polym Chem 49:72–81
19. Yuan Y, Michinobu T (2011) Microwave-assisted TCNE/TCNQ addition to poly(thienyleneethynylene) derivative for construction of donor-acceptor chromophores. J Polym Sci A Polym Chem 49:1013–1020
20. Fujita H, Tsuboi K, Michinobu T (2011) High-yielding alkyne–tetracyanoethylene addition reactions: a powerful tool for analyzing alkyne-linked conjugated polymer structures. Macromol Chem Phys 212:1758–1766
21. Michinobu T, May JC, Lim JH, Boudon C, Gisselbrecht JP, Seiler P, Gross M, Biaggio I, Diederich F (2005) A new class of organic donor–acceptor molecules with large third-order optical nonlinearities. Chem Commun 737–739
22. Michinobu T, Boudon C, Gisselbrecht JP, Seiler P, Frank B, Moonen NNP, Gross M, Diederich F (2006) Donor-substituted 1,1,4,4-tetracyanobutadienes (TCBDs): new chromophores with efficient intramolecular charge-transfer interactions by atom-economic synthesis. Chem Eur J 12:1889–1905
23. Kolb HC, Finn MG, Sharpless KB (2001) Click chemistry: diverse chemical function from a few good reactions. Angew Chem Int Ed 40:2004–2021
24. Michinobu T (2008) Click-type reaction of aromatic polyamines for improvement of thermal and optoelectronic properties. J Am Chem Soc 130:14074–14075
25. Yuan Y, Michinobu T (2011) Energy level tuning of polythiophene derivative by click chemistry-type postfunctionalization of side chain alkynes. J Polym Sci A Polym Chem 49:225–233
26. Onuma KI, Kai Y, Yasuoka N, Kasai N (1975) The crystal and molecular structure of trans-bis(trimethylphosphine)propynyl-1-(4′-dicyanomethylene-cyclohexa-2′,5′-dien-1-yliden)-3,3-dicyano-2-methyl-prop-2-en-1-ylplatinum, a reaction product of trans-bis(trimethylphosphine)bis(propynyl)platinum and 7,7,8,8-tetracyanoquinodimethane. Bull Chem Soc Jpn 48:1696–1700

27. Kivala M, Boudon C, Gisselbrecht JP, Seiler P, Gross M, Diederich F (2007) A novel reaction of 7,7,8,8-tetracyanoquinodimethane (TCNQ): charge-transfer chromophores by [2+2] cycloaddition with alkynes. Chem Commun 4731–4733
28. Reutenauer P, Kivala M, Jarowski PD, Boudon C, Gisselbrecht JP, Gross M, Diederich F (2007) New strong organic acceptors by cycloaddition of TCNE and TCNQ to donor-substituted cyanoalkynes. Chem Commun 4898–4900
29. Butler P, Manning AR, AcAdam CJ, Simpson J (2008) The reactions of some σ-alkynylnickel complexes with 7,7,8,8-tetracyanoquinodimethane. J Organomet Chem 693:381–392
30. Bruce MI, Cole MI, Parker CR, Skelton BW, White AH (2008) Synthesis and some reactions of the heterometallic C7 complex Cp*(dppe)Ru $C{\equiv}CC{\equiv}CC{\equiv}CC\{Co_3(\mu\text{-dppm})(CO)_7\}$. Organometallics 27:3352–3367
31. Kivala M, Boudon C, Gisselbrecht JP, Enko B, Seiler P, Müller IB, Langer N, Jarowski PD, Gescheidt G, Diederich F (2009) Organic super-acceptors with efficient intramolecular charge-transfer interactions by [2+2] cycloadditions of TCNE, TCNQ, and F_4-TCNQ to donor-substituted cyanoalkynes. Chem Eur J 15:4111–4123
32. Washino Y, Tsuboi K, Michinobu T (2011) Simultaneous formation of donor-acceptor chromophores and cross-linking for electro-optic polymer materials. J Photopolym Sci Technol 24:305–309
33. Washino Y, Michinobu T (2011) Application of alkyne–TCNQ addition reaction to polymerization. Macromol Rapid Commun 32:644–648
34. Washino Y, Murata K, Ashizawa M, Kawauchi S, Michinobu T (2011) Creation of persistent charge-transfer interactions in TCNQ polyester. Polym J 43:364–369
35. Li Y, Tsuboi K, Michinobu T, Ishida Y, Hirai T, Hayakawa T, Kakimoto MA (2010) Efficient synthesis of block copolymers bearing donor-acceptor chromophores for second-order nonlinear optical applications. J Photopolym Sci Technol 23:337–342
36. Li Y, Michinobu T (2010) Sequential double click reactions: a highly efficient post-functionalization method for optoelectronic polymers. Polym Chem 1:72–74
37. Li Y, Tsuboi K, Michinobu T (2010) Double click synthesis and second-order nonlinearities of polystyrenes bearing donor–acceptor chromophores. Macromolecules 42:5277–5286
38. Hamciuc E, Hamciuc C, Cazacu M, Ignat M, Zarnescu G (2009) Polyimide–polydimethylsiloxane copolymers containing nitrile groups. Eur Poly J 45:182–190
39. Kato SI, Diederich F (2010) Non-planar push–pull chromophores. Chem Commun 46:1994–2006
40. Morimoto M, Murata K, Michinobu T (2011) Photochemical control of a highly efficient addition reaction between electron-rich alkynes and tetracyanoethylene. Chem Commun 47:9819–9821
41. Esembeson B, Scimeca ML, Michinobu T, Diederich F, Biaggio I (2008) A high-optical quality supramolecular assembly for third-order integrated nonlinear optics. Adv Mater 20:4584–4587
42. Kato SI, Kivala M, Schweizer WB, Boudon C, Gisselbrecht JP, Diederich F (2009) Origin of intense intramolecular charge-transfer interactions in nonplanar push–pull chromophores. Chem Eur J 15:8687–8691
43. Jordan M, Kivala M, Boudon C, Gisselbrecht JP, Schweizer WB, Seiler P, Diederich F (2011) Switching the regioselectivity in cycloaddition-retro-electrocyclizations between donor-activated alkynes and the electron-accepting olefins TCNE and TCNQ. Chem Asian J 6:396–401
44. Tang X, Liu W, Wu J, Lee CS, You J, Wang P (2010) Synthesis, crystal structures, and photophysical properties of triphenylamine-based multicyano derivatives. J Org Chem 75:7273–7278